# STRESS INTENSITY FACTORS OF A SEMI-ELLIPTICAL CRACK IN A HOLLOW CYLINDER

Shiuh-Chuan Her and Hao-Hi Chang
*Department of Mechanical Engineering, Yuan Ze University, Chung-Li, Taiwan, R.O.C.*
*E-mail: mesch@saturn.yzu.edu.tw*

ICETI-2014 J1071_SCI
No. 15-CSME-33, E.I.C. Accession 3808

## ABSTRACT

In this investigation, the weight function method was employed to calculate stress intensity factors for semi-elliptical surface crack in a hollow cylinder. A uniform stress and a linear stress distribution were used as the two references to determine the weight functions. These two factors were obtained by a three-dimensional finite element method which employed singular elements along the crack front and regular elements elsewhere. The weight functions were then applied to a wide range of semi-elliptical surface crack subjected to non-linear loadings. The results were validated against finite element data and compared with other analyses. In the parametric study, the effects of the ratio of the surface crack depth to length ranged from 0.2 to 1.0 and the ratio of the crack depth to the wall thickness ranged from 0.2 to 0.8 on stress intensity factors were investigated.

**Keywords:** semi-elliptical surface crack; weight function; stress intensity factor.

# FACTEURS D'INTENSITÉ DE STRESS D'UNE FISSURE SEMI-ELLIPTIQUE À L'INTÉRIEUR D'UN CYLINDRE CREUX

## RÉSUMÉ

Au cours de cette recherche, la méthode de fonction de pondération a été employée pour calculer les facteurs d'intensité de stress d'une fissure sur une surface semi-elliptique d'un cylindre creux. Des distributions de stress uniforme et de stress semi-linéaire ont été utilisées comme les deux références pour déterminer la fonction de pondération. Ces deux facteurs d'intensité de stress de référence ont été obtenus par la méthode des éléments finis en trois dimensions, laquelle a employé des éléments singuliers le long du devant de la fissure et des éléments réguliers ailleurs. La fonction de pondération a alors été appliquée à une vaste gamme de fissures de surface semi-elliptique soumise à des chargements nonlinéaires. Les résultats ont été validés par rapport à des données d'éléments finis, et comparés à d'autres analyses. Dans l'étude des paramètres, on a investigué sur les facteurs d'intensité de stress, les effets de la moyenne des profondeurs des fissures de surface dont la longueur s'étendait de 0,2 à 1,0, et la moyenne de profondeur de la fissure à l'épaisseur de la paroi qui s'étendait de 0,2 à 0,8.

**Mots-clés :** fissure sur une surface semi-elliptique; fonction de pondération; facteur d'intensité de stress.

## 1. INTRODUCTION

Hollow cylinders are widely used as pressure vessels and pipes in many engineering applications such as nuclear and chemical industries. Semi-elliptical surface cracks are commonly found in the manufacturing process and in the product's service life. In the manufacturing process and during the service life of the product, a flaw may initiate an internal or an external boundary in the cylinder. Structures often fail by the extension of surface flaws. In practical applications, the determination of stress intensity factors for various stress distributions along the pipe wall thickness is necessary to assess their load carrying capacity, remaining service life and the safety of cylindrical components against fracture failure. The weight function method proposed by Bueckner [1] and Rice [2] is a powerful technique for the calculation of stress intensity factors. The unique feature of the weight function method is that once the weight function for a particular cracked body has been determined, the stress intensity factor for any loading applied to that cracked body can be obtained by integrating the product of the loading and the weight function. The weight function depends only on the geometry of the cracked body. Thus, the weight function is a very efficient technique to calculate stress intensity factors.

Since the introduction of the weight function concept to crack problems by Bueckner [1] and Rice [2], many applications have emerged for the calculation of stress intensity factors. Zheng et al. [3, 4] derived stress intensity factors for semielliptical cracks in a thick-wall cylinder from a general weight function and two reference stress intensity factors. For surface cracks in a flat plate, Shen and Glinka [5], Wang and Lambert [6–8] have generated approximate weights for semi-elliptical surface cracks in finite thickness plates. A weight function with a matrix structure was proposed by Beghini et al. [9] to account for coupling effects between modes I and II, for 2D subsurface cracks under general loading conditions. Montenegro et al. [10] employed weight function methodology for the assessment of embedded and surface irregular plane cracks. Anderson and Glinka [11] presented a weight function integration technique for part-through surface and corner cracks subjected to mode I loading. Teh and Brennan [12] evaluated stress intensity factors for mode I edge cracks emanating from V-notches in finite strips using weight functions. Kim and Lee [13] calculated stress intensity factors using the weight function method for a patched crack with debonding region. Guo et al. [14] derived an accurate weight function for a single edge crack originating from the weld toe of a T-plate.

In this investigation, the weight function method was employed to calculate stress intensity factors for semi-elliptical surface crack in a hollow cylinder. The weight functions at both the deepest and surface points in the semi-elliptical surface crack were derived. The coefficients of the weight functions were determined from two reference stress intensity factor solutions obtained by finite element method with constant and linearly varying face loads. Validation of the derived weight functions was conducted using stress intensity factors results from the literature.

## 2. DERIVATION OF WEIGHT FUNCTIONS

Consider a semi-elliptical surface crack in a hollow cylinder as shown in Fig.1, subjected to a stress field, which applies on the crack face and varies in the $x$-direction. The stress intensity factor at any point can be calculated by integrating the product of the weight function and the stress distribution. Glinka and Shen [15] presented the following general weight function that can be used for a variety of crack configuration subjected to one-dimensional mode I stress field:

$$m(x,a) = \frac{2}{\sqrt{2\pi(a-x)}}\left[1 + M_1\left(1-\frac{x}{a}\right)^{1/2} + M_2\left(1-\frac{x}{a}\right) + M_3\left(1-\frac{x}{a}\right)^{3/2}\right] \quad (1)$$

where $M_i$ $(i = 1,2,3)$ are parameters that depend only on the geometrical configuration of the cracked body. The weight function singularity term corresponds to the first term. The subsequent terms are merely a series

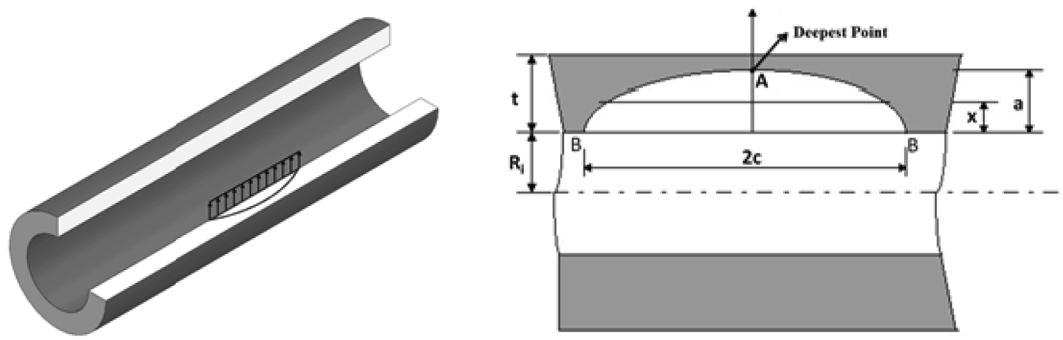


Fig. 1. Hollow cylinder with semi-elliptical surface crack.

of representation of the function.

In this work, the general weight function (1) was adopted for the semi-elliptical surface crack. For the deepest point A, the weight function is given as

$$m_A(x,a) = \frac{2}{\sqrt{2\pi(a-x)}}\left[1 + M_{1A}\left(1-\frac{x}{a}\right)^{1/2} + M_{2A}\left(1-\frac{x}{a}\right) + M_{3A}\left(1-\frac{x}{a}\right)^{3/2}\right] \tag{2}$$

For the surface point B, the weight function is written as

$$m_B(x,a) = \frac{2}{\sqrt{2\pi(a-x)}}\left[1 + M_{1B}\left(1-\frac{x}{a}\right)^{1/2} + M_{2B}\left(1-\frac{x}{a}\right) + M_{3B}\left(1-\frac{x}{a}\right)^{3/2}\right] \tag{3}$$

Physically, the weight functions $m_A$ and $m_B$ represent stress intensity factors at deepest point A and surface point B, respectively, for a unit line load at $x$ as shown in Fig. 1. In the case of a distributed stress field $\sigma(x)$ which is a function of coordinate $x$ only, the stress intensity factor for the deepest point A and surface point B can be obtained by integrating the product of the weight function and the stress distribution as follows:

$$K_A = \int_0^a m_A(x,a)\sigma(x)dx \tag{4}$$

$$K_B = \int_0^a m_B(x,a)\sigma(x)dx \tag{5}$$

In order to calculate stress intensity factors, it is necessary to determine parameters $M_{iA}$ and $M_{iB}$ in weight functions $m_A$ and $m_B$, respectively. The parameters $M_{iA}$ and $M_{iB}$ can be derived [4] using two reference stress intensity factors and some properties of the weight functions. In this study, stress intensity factors obtained for the constant and linear increasing loads were chosen as the two references:

$$\sigma(x) = \sigma_0 \quad \text{constant loads} \tag{6}$$

$$\sigma(x) = \sigma_0\left(\frac{x}{a}\right) \quad \text{linearly increasing loads} \tag{7}$$

The stress intensity factors calculated for applied loads Eqs. (6) and (7) were expressed in terms of the geometry correction factors $Y_i$.

For the deepest point A:

$$K_0^A = \sigma_0\sqrt{\frac{\pi a}{Q}}Y_0 \quad \text{constant loads} \tag{8}$$

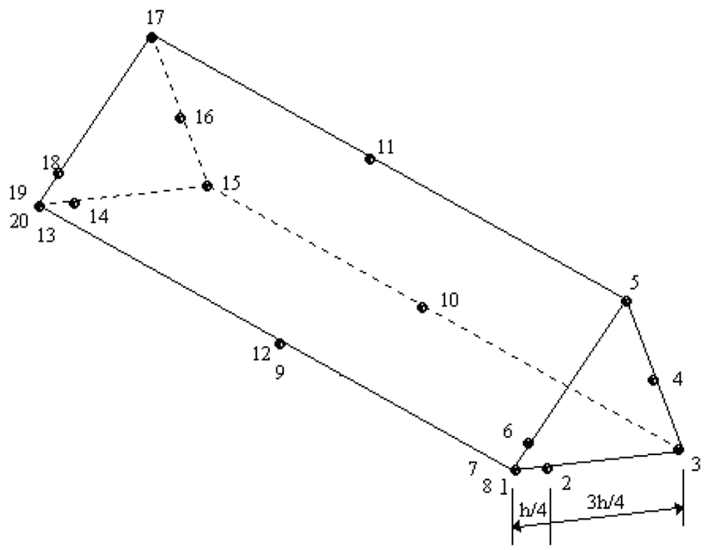


Fig. 2. Quarter point element.

$$K_1^A = \sigma_0 \sqrt{\frac{\pi a}{Q}} Y_1 \quad \text{linearly increasing loads} \tag{9}$$

For the surface point B:

$$K_0^B = \sigma_0 \sqrt{\frac{\pi a}{Q}} F_0 \quad \text{constant loads} \tag{10}$$

$$K_1^B = \sigma_0 \sqrt{\frac{\pi a}{Q}} F_1 \quad \text{linearly increasing loads} \tag{11}$$

$$Q = 1 + 1.464 \left(\frac{a}{c}\right)^{1.65}$$

where $Q$ is the shape factor for an ellipse [16]; $a$ and $c$ denote the depth and half length of the semi-elliptical surface crack, respectively.

The two reference stress intensity factors $K_0^A$, $K_0^B$ and $K_1^A$, $K_1^B$ were obtained using the finite element method. The finite element analysis was conducted using ANSYS with 20 nodes 3-D solid elements. Three-dimensional finite elements were employed to model the symmetric quarter of a hollow cylinder containing a semi-elliptical surface crack. In the vicinity of the crack tip, three-dimensional prism elements as shown in Fig. 2 with one mid-side node at the quarter point and coalescing nodes along one side were used to model the square root singularity at the crack tip. A typical finite element mesh is shown in Fig. 3. The loads were directly applied to the crack face. The stress intensity factor for model I was calculated from the tensile stress ahead of the crack tip

$$K_I = \sigma_y \sqrt{2\pi r}$$

where $\sigma_y$ and $r$ are the tensile stress and distance to the crack tip, respectively.

The stress intensity factors of the deepest and surface points for the constant loads and linear loads were obtained for a variety of geometric configuration. The ratio of crack depth to length $a/c$ is varied from 0.2 to 1; the ratio of the crack depth to the cylinder thickness $a/t$ varying from 0.2 to 0.8; while the ratio of inner radius to thickness is fixed to $R_i/t = 4$. The stress intensity factors obtained from FEM results

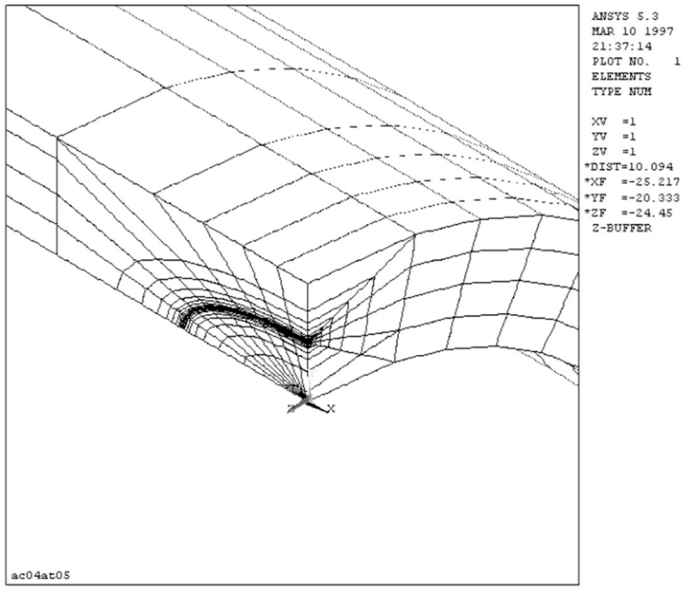


Fig. 3. Finite element mesh.

are normalized by $\sigma_0\sqrt{\pi a/Q}$. The normalized stress intensity factors for constant loads at the deepest and surface points are as follows:

$$\frac{K_0^A}{\sigma_0\sqrt{\pi\, a/Q}} = Y_0; \quad \frac{K_0^B}{\sigma_0\sqrt{\pi\, a/Q}} = F_0 \tag{12}$$

The normalized stress intensity factors for linearly increasing loads at the deepest and surface points are as follows:

$$\frac{K_1^A}{\sigma_0\sqrt{\pi\, a/Q}} = Y_1; \quad \frac{K_1^B}{\sigma_0\sqrt{\pi\, a/Q}} = F_1 \tag{13}$$

The normalized stress intensity factors $Y_0, Y_1, F_0, F_1$ obtained by the finite element method are presented in Table 1 for a variety of crack depths $a/t$ and aspect ratios $a/c$. Using least square curve fitting, the normalized stress intensity factors $Y_0, Y_1, F_0, F_1$ can be expressed in a polynomial function of crack depths $a/t$ and aspect ratios $a/c$ as follows:

$$\begin{aligned}
&Y_0 = A_0 + A_1(a/t)^2 + A_2(a/t)^4 \\
&A_0 = 0.741 + 2.473(a/c) - 5.162(a/c)^2 + 1.286(a/c)^3 + 4.491(a/c)^4 - 2.802(a/c)^5 \\
&A_1 = 4.75 - 21.609(a/c) + 33.998(a/c)^2 - 4.692(a/c)^3 - 27.85(a/c)^4 + 15.448(a/c)^5 \\
&A_2 = -1.817 + 8.727(a/c) - 13.224(a/c)^2 + 0.724(a/c)^3 + 10.039(a/c)^4 - 4.34(a/c)^5
\end{aligned} \tag{14}$$

$$\begin{aligned}
&Y_1 = B_0 + B_1(a/t)^2 + B_2(a/t)^4 \\
&B_0 = 0.571 + 0.933(a/c) - 2.487(a/c)^2 + 1.032(a/c)^3 + 2.507(a/c)^4 - 1.862(a/c)^5 \\
&B_1 = 1.614 - 12.493(a/c) + 32.177(a/c)^2 - 14.824(a/c)^3 - 33.45(a/c)^4 + 26.942(a/c)^5 \\
&B_2 = -0.381 + 9.015(a/c) - 31.062(a/c)^2 + 18.516(a/c)^3 + 35.221(a/c)^4 - 31.108(a/c)^5
\end{aligned} \tag{15}$$

Table 1. Two reference normalized stress intensity factors with constant loading and linear loading applied to the crack surface.

| a/c | a/t | Deepest point A $\frac{K_A}{\sigma_0\sqrt{\pi a/Q}}$ | | Surface point B $\frac{K_B}{\sigma_0\sqrt{\pi a/Q}}$ | |
|---|---|---|---|---|---|
| | | $Y_0$ constant loading | $Y_1$ linear loading | $F_0$ constant loading | $F_1$ linear loading |
| 0.2 | 0.2 | 1.107 | 0.68 | 0.606 | 0.078 |
| | 0.5 | 1.393 | 0.753 | 0.803 | 0.144 |
| | 0.8 | 1.926 | 0.976 | 1.193 | 0.252 |
| 0.4 | 0.2 | 1.1 | 0.667 | 0.785 | 0.119 |
| | 0.5 | 1.234 | 0.718 | 0.929 | 0.173 |
| | 0.8 | 1.44 | 0.818 | 1.224 | 0.254 |
| 0.6 | 0.2 | 1.032 | 0.649 | 0.849 | 0.138 |
| | 0.5 | 1.145 | 0.703 | 0.956 | 0.179 |
| | 0.8 | 1.343 | 0.801 | 1.263 | 0.244 |
| 0.8 | 0.2 | 1.014 | 0.662 | 0.999 | 0.167 |
| | 0.5 | 1.099 | 0.65 | 1.076 | 0.199 |
| | 0.8 | 1.22 | 0.783 | 1.297 | 0.242 |
| 1.0 | 0.2 | 1.029 | 0.693 | 1.116 | 0.193 |
| | 0.5 | 1.045 | 0.698 | 1.195 | 0.217 |
| | 0.8 | 1.1 | 0.754 | 1.306 | 0.242 |

$$\begin{aligned}
&F_0 = C_0 + C_1(a/t)^2 + C_2(a/t)^4 \\
&C_0 = 0.021 + 4.22(a/c) - 7.721(a/c)^2 + 2.312(a/c)^3 + 7.382(a/c)^4 - 5.116(a/c)^5 \\
&C_1 = -0.159 + 6.341(a/c) - 13.16(a/c)^2 + 2.569(a/c)^3 + 10.814(a/c)^4 - 5.984(a/c)^5 \\
&C_2 = 3.126 - 19.575(a/c) + 37.326(a/c)^2 - 8.179(a/c)^3 - 32.222(a/c)^4 + 19.372(a/c)^5
\end{aligned} \tag{16}$$

$$\begin{aligned}
&F_1 = D_0 + D_1(a/t)^2 + D_2(a/t)^4 \\
&D_0 = -0.043 + 0.761(a/c) - 1.207(a/c)^2 + 0.288(a/c)^3 + 1.127(a/c)^4 - 0.738(a/c)^5 \\
&D_1 = 0.273 + 0.707(a/c) - 2.296(a/c)^2 + 0.848(a/c)^3 + 2.082(a/c)^4 - 1.476(a/c)^5 \\
&D_2 = 0.189 - 2.096(a/c) + 4.637(a/c)^2 - 1.49(a/c)^3 - 4.316(a/c)^4 + 2.992(a/c)^5
\end{aligned} \tag{17}$$

### 2.1. Weight Function for the Deepest Point A

Substituting Eqs. (2), (6), (7) into Eq. (4) leads to the following two equations containing parameters $M_{iA}$:

$$K_0^A = \sigma_0\sqrt{\frac{\pi a}{Q}}Y_0 = \int_0^a \frac{2\sigma_0}{\sqrt{2\pi(a-x)}}\left[1 + M_{1A}\left(1-\frac{x}{a}\right)^{1/2} + M_{2A}\left(1-\frac{x}{a}\right)^{1} + M_{3A}\left(1-\frac{x}{a}\right)^{3/2}\right]dx \tag{18}$$

$$K_1^A = \sigma_0\sqrt{\frac{\pi a}{Q}}Y_1 = \int_0^a \sigma_0\left(\frac{x}{a}\right)\frac{2}{\sqrt{2\pi(a-x)}}\left[1 + M_{1A}\left(1-\frac{x}{a}\right)^{1/2} + M_{2A}\left(1-\frac{x}{a}\right)^{1} + M_{3A}\left(1-\frac{x}{a}\right)^{3/2}\right]dx \tag{19}$$

As observed by Fett et al. [17] and Shen [5], the third equation for finding parameters $M_{1A}$, $M_{2A}$ and $M_{3A}$ is that the second derivative of the weight function be zero at $x = 0$

$$\left.\frac{\partial^2 m_A}{\partial x^2}\right|_{x=0} = 0 \tag{20}$$

Thus, parameters $M_{1A}$, $M_{2A}$ and $M_{3A}$ can be determined by solving Eqs. (18), (19) and (20) as follows:

$$M_{1A} = \frac{2\pi}{\sqrt{2Q}}(-Y_0 + 3Y_1) - \frac{24}{5} \tag{21}$$

$$M_{2A} = 3 \tag{22}$$

$$M_{3A} = \frac{6\pi}{\sqrt{2Q}}(Y_0 - 2Y_1) + \frac{8}{5} \tag{23}$$

where $Y_0$ and $Y_1$ have been given by closed form expressions in Eqs. (14) and (15), respectively.

### 2.2. Weight Function for the Surface Point B

Substituting Eqs. (3), (6), (7) into Eq. (5) leads to the following two equations containing parameters $M_{iB}$:

$$K_0^B = \sigma_0\sqrt{\frac{\pi a}{Q}}F_0 = \int_0^a \sigma_0 \frac{2}{\sqrt{\pi x}}\left[1 + M_{1B}\left(\frac{x}{a}\right)^{1/2} + M_{2B}\left(\frac{x}{a}\right) + M_{3B}\left(\frac{x}{a}\right)^{3/2}\right]dx \tag{24}$$

$$K_1^B = \sigma_0\sqrt{\frac{\pi a}{Q}}F_1 = \int_0^a \sigma_0\left(\frac{x}{a}\right) \frac{2}{\sqrt{\pi x}}\left[1 + M_{1B}\left(\frac{x}{a}\right)^{1/2} + M_{2B}\left(\frac{x}{a}\right) + M_{3B}\left(\frac{x}{a}\right)^{3/2}\right]dx \tag{25}$$

The third equation for evaluating parameters $M_{1B}$, $M_{2B}$ and $M_{3B}$ is that the weight function equals to zero at $x = a$, i.e.

$$m_B(x,a)|_{x=a} = 1 + M_{1B} + M_{2B} + M_{3B} = 0 \tag{26}$$

Thus, parameters $M_{1B}$, $M_{2B}$ and $M_{3B}$ can be determined by solving Eqs. (24), (25) and (26) as follows:

$$M_{1B} = \frac{3\pi}{\sqrt{Q}}(2F_0 - 5F_1) - 8 \tag{27}$$

$$M_{2B} = \frac{15\pi}{\sqrt{Q}}(-F_0 + 3F_1) + 15 \tag{28}$$

$$M_{3B} = \frac{3\pi}{\sqrt{Q}}(3F_0 - 10F_1) - 8 \tag{29}$$

where $F_0$ and $F_1$ have been given by closed form expressions in Eqs. (16) and (17), respectively.

## 3. VERIFICATIONS

To verify the accuracy of the derived weight functions, stress intensity factors for several power-law loadings applied to the semi-elliptical crack surface were calculated for the deepest point A and surface point B by using Eqs. (4) and (5). The results were compared with available reference data [18].

$$\sigma(x) = \sigma_0\left(\frac{x}{a}\right)^n, \quad n = 1, 3 \tag{30}$$

### 3.1. Stress Intensity Factors for the Deepest Point A

The stress intensity factors for the deepest point A were calculated by substituting the applied loading from Eq. (30) and the weight function from Eqs. (2), (21), (22) and (23) into Eq. (4).

*Case 1*: $n = 1$, $\sigma(x) = \sigma_0(x/a)$ linear loading:

$$\frac{K_A}{\sigma_0\sqrt{\pi a/Q}} = \frac{\sqrt{2Q}}{\pi}\left(\frac{4}{3} + \frac{1}{2}M_{1A} + \frac{4}{15}M_{2A} + \frac{1}{6}M_{3A}\right) = Y_1 \tag{31}$$

Table 2. Comparison of the weight function based normalized stress intensity factors for deepest and surface points to the finite element data [18] with linear loading applied to the crack surface.

| a/c | a/t | Deepest point A $\frac{K_A}{\sigma_0\sqrt{\pi a/Q}}$ | | | Surface point B $\frac{K_B}{\sigma_0\sqrt{\pi a/Q}}$ | | |
|---|---|---|---|---|---|---|---|
| | | present | Raju and Newman [18] | Difference % | present | Raju and Newman[18] | Difference % |
| 0.2 | 0.2 | 0.68 | 0.666 | 2.102 | 0.078 | 0.079 | 1.265 |
| | 0.5 | 0.753 | 0.776 | 2.963 | 0.144 | 0.141 | 2.128 |
| | 0.8 | 0.976 | 0.996 | 2.008 | 0.252 | 0.262 | 3.816 |
| 0.4 | 0.2 | 0.667 | 0.666 | 0.15 | 0.119 | 0.123 | 3.252 |
| | 0.5 | 0.718 | 0.715 | 0.42 | 0.173 | 0.174 | 0.574 |
| | 0.8 | 0.818 | 0.828 | 1.207 | 0.254 | 0.263 | 3.422 |
| 0.6 | 0.2 | 0.649 | * | * | 0.138 | * | * |
| | 0.5 | 0.703 | * | * | 0.179 | * | * |
| | 0.8 | 0.801 | * | * | 0.244 | * | * |
| 0.8 | 0.2 | 0.662 | * | * | 0.167 | * | * |
| | 0.5 | 0.65 | * | * | 0.199 | * | * |
| | 0.8 | 0.783 | * | * | 0.242 | * | * |
| 1.0 | 0.2 | 0.693 | 0.713 | 2.805 | 0.193 | 0.194 | 0.515 |
| | 0.5 | 0.698 | 0.726 | 3.856 | 0.217 | 0.214 | 1.402 |
| | 0.8 | 0.754 | 0.768 | 1.822 | 0.242 | 0.248 | 2.419 |

$*$ Not available in [18].

*Case 2*: $n = 3$, $\sigma(x) = \sigma_0(x/a)^3$ cubic loading:

$$\frac{K_A}{\sigma_0\sqrt{\pi a/Q}} = \frac{\sqrt{2Q}}{\pi}\left(\frac{32}{35} + \frac{1}{4}M_{1A} + \frac{32}{315}M_{2A} + \frac{1}{20}M_{3A}\right) \tag{32}$$

### 3.2. Stress Intensity Factors for the Surface Point B

The stress intensity factors for the surface point B were calculated by substituting the applied loading from Eq. (30) and the weight function from Eqs. (3), (27), (28) and (29) into Eq. (5).

*Case 1*: $n = 1$, $\sigma(x) = \sigma_0(x/a)$ linear loading:

$$\frac{K_B}{\sigma_0\sqrt{\pi a/Q}} = \frac{\sqrt{Q}}{\pi}\left(\frac{4}{3} + M_{1B} + \frac{4}{5}M_{2B} + \frac{2}{3}M_{3B}\right) = F_1 \tag{33}$$

*Case 2*: $n = 3$, $\sigma(x) = \sigma_0(x/a)^3$ cubic loading:

$$\frac{K_B}{\sigma_0\sqrt{\pi a/Q}} = \frac{\sqrt{Q}}{\pi}\left(\frac{4}{7} + \frac{1}{2}M_{1B} + \frac{4}{9}M_{2B} + \frac{2}{5}M_{3B}\right) \tag{34}$$

The normalized stress intensity factors obtained from Eqs. (31)–(34) for a variety of crack depths $a/t$ and aspect ratios $a/c$ are compared with the results by Raju and Newman [18]. Table 2 shows normalized stress intensity factors for the deepest and surface points with linear loading applied to the semi-elliptical crack surface. In the case of cubic loading, the normalized stress intensity factors for the deepest and surface points are presented in Table 3. The comparisons of normalized stress intensity factors calculated by using Eqs. (31)–(34) to the finite element data by Raju and Newman [18] are in good agreement. The difference between the present approach using weight function and the finite element data [18] is less than 5%. The variation of normalized stress intensity factors with the crack depths $a/t$ and crack aspect ratios $a/c$for the

Table 3. Comparison of the weight function based normalized stress intensity factors for deepest and surface points to the finite element data [18] with cubic loading applied to the crack surface.

| a/c | a/t | Deepest point A $\frac{K_A}{\sigma_0\sqrt{\pi a/Q}}$ | | | Surface point B $\frac{K_B}{\sigma_0\sqrt{\pi a/Q}}$ | | |
|---|---|---|---|---|---|---|---|
| | | present | Raju and Newman [18] | Difference % | present | Raju and Newman [18] | Difference % |
| 0.2 | 0.2 | 0.436 | 0.426 | 2.347 | 0.011 | 0.01 | 10 |
| | 0.5 | 0.447 | 0.46 | 2.826 | 0.029 | 0.028 | 3.571 |
| | 0.8 | 0.545 | 0.542 | 0.554 | 0.057 | 0.059 | 3.389 |
| 0.4 | 0.2 | 0.432 | 0.439 | 1.594 | 0.021 | 0.021 | 0 |
| | 0.5 | 0.451 | 0.454 | 0.66 | 0.037 | 0.036 | 2.778 |
| | 0.8 | 0.499 | 0.509 | 1.964 | 0.059 | 0.059 | 0 |
| 0.6 | 0.2 | 0.435 | * | * | 0.058 | * | * |
| | 0.5 | 0.461 | * | * | 0.041 | * | * |
| | 0.8 | 0.517 | * | * | 0.055 | * | * |
| 0.8 | 0.2 | 0.456 | * | * | 0.034 | * | * |
| | 0.5 | 0.428 | * | * | 0.045 | * | * |
| | 0.8 | 0.528 | * | * | 0.052 | * | * |
| 1.0 | 0.2 | 0.501 | 0.511 | 1.956 | 0.038 | 0.037 | 2.71 |
| | 0.5 | 0.499 | 0.515 | 3.106 | 0.045 | 0.043 | 4.651 |
| | 0.8 | 0.529 | 0.536 | 1.306 | 0,051 | 0.05 | 2 |

$*$ Not available in [18].

deepest and surface points with linear loading applied to the crack surface are plotted in Figs. 4 and 5, respectively. It can be observed that stress intensity factors for both the deepest and surface points increase with the increase in the crack depth $a/t$. The stress intensity factor for the deepest point is decreasing with the increase in the crack aspect ratio $a/c$, while the stress intensity factor the surface point increases with the increase in the crack aspect ratio.

## 4. STRESS INTENSITY FACTOR OF PRESSURIZED HOLLOW CYLINDER

A thick-wall cylinder with an internal semi-elliptical surface crack is subjected to internal pressure $p$. The stress intensity factor due to the internal pressure can be calculated by using the weight functions (2) and (3) and the hoop stress developed in the cylinder. For the pressured hollow cylinder, the hoop stress is given as [4]:

$$\sigma_{\text{hoop}}(x) = \frac{pR_i^2}{t\,(2R_i+t)}\left[1+\left(\frac{R_i+t}{R_i+x}\right)^2\right] \tag{35}$$

where $R_i$ and $t$ are the inner radius and thickness of the hollow cylinder.

As the internal pressure $p$ of the hollow cylinder is included, the resulting loads acted on the semi-elliptical crack face can be written as

$$\sigma(x) = p\left\{1+\frac{R_i^2}{t\,(2R_i+t)}\left[1+\left(\frac{R_i+t}{R_i+x}\right)^2\right]\right\} \tag{36}$$

Substituting the weight functions (2) and (3) and the stress applied on the crack face Eq. (36) into Eqs. (4) and (5), stress intensity factors of a pressured hollow cylinder can be obtained.

The normalized stress intensity for the deepest point with inner radius to thickness ratio $R_i/t = 4$, crack depth $a/t = 0.5$and crack aspect ratio $a/c = 0.4$ calculated by weight function is given as

$$\frac{K_A}{p\sqrt{\pi a/Q}} = 6.396 \tag{37}$$

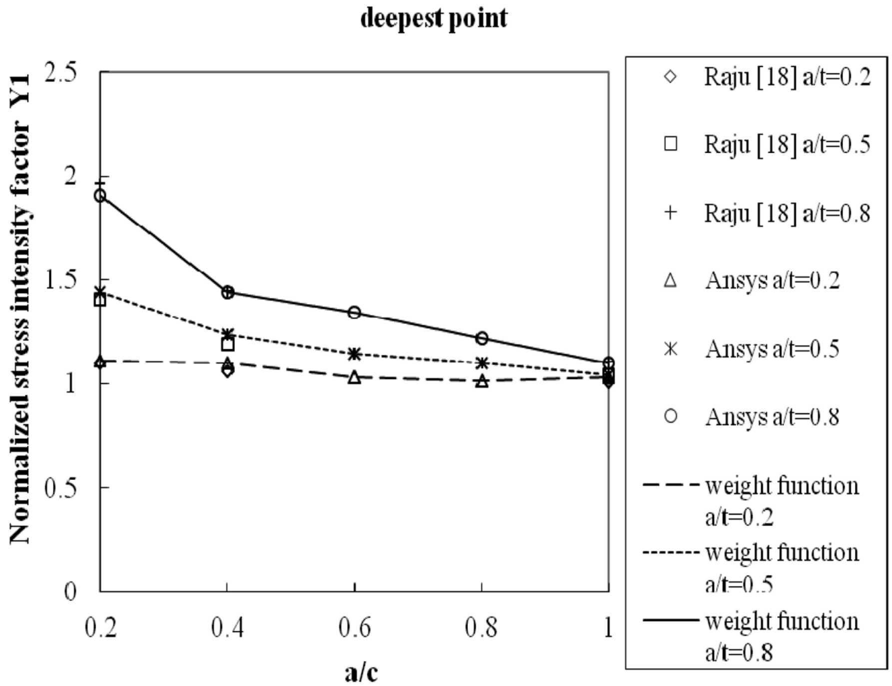


Fig. 4. Normalized stress intensity factor for the deepest point with linear loading acted on the crack surface.

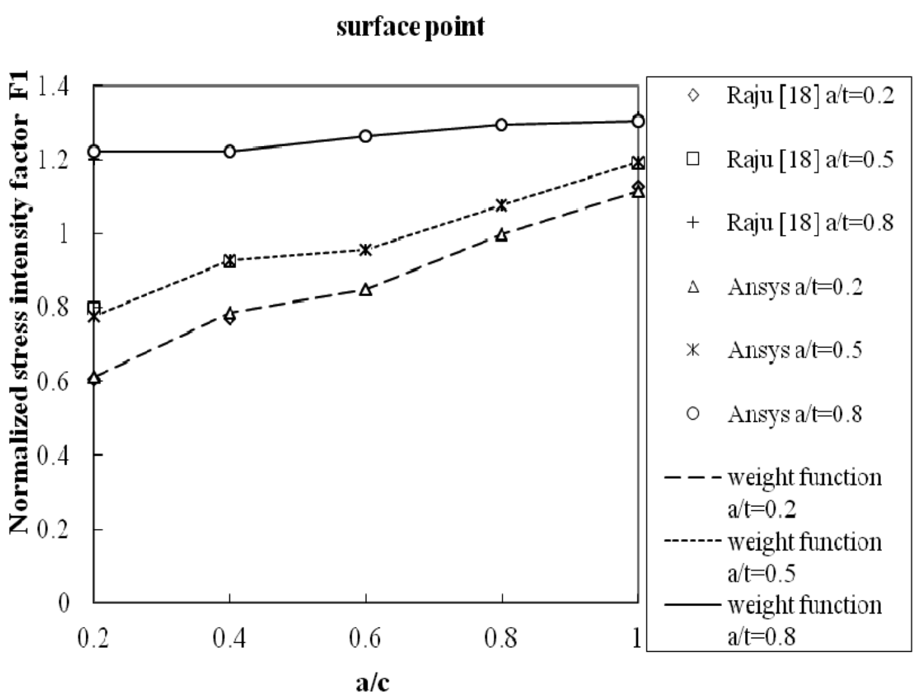


Fig. 5. Normalized stress intensity factor for the surface point with linear loading acted on the crack surface.

While the normalized stress intensity for the deepest point using the finite element method is

$$\frac{K_A}{p\sqrt{\pi a/Q}} = 6.168 \tag{38}$$

The difference of the stress intensity factor for a semi-elliptical surface crack in a pressurized thick-wall cylinder calculated by using the weight function and finite element method is about 3.7%.

## 5. CONCLUSIONS

Stress intensity factors for a hollow cylinder with a semi-elliptical surface crack were derived by using the weight function method. Two reference stress intensity factors for constant loading and linear loading applied to the crack face were employed to determine the parameters of the weight functions. Stress intensity factors for two power-law loadings acted on the crack surface were then calculated for a variety of crack depths and crack aspect ratios. Good agreement with available literature data was achieved over the range of crack depths $0.2 \leq a/t \leq 0.8$ and crack aspect ratios $0.2 \leq a/c \leq 1.0$. Finally, stress intensity factor for internal semi-elliptical surface crack in a hollow cylinder subjected to internal pressure was calculated and verified with the finite element result. The derived weight functions provide a rapid computation of stress intensity factors for cracks subjected to complex loadings.

## REFERENCES


1. Bueckner, H.F., "A novel principle for the computation of stress intensity factor", *Zeit. Angew Math. Mech.*, Vol. 50, pp. 129–146, 1970.
2. Rice, J.R., "Some remarks on elastic crack-tip stress fields", *International Journal of Solids and Structures*, Vol. 8, pp. 751–758, 1972.
3. Zheng, X.J., Kiciak, A. and Glinka, G., "Weight functions and stress intensity factors for internal surface semi-elliptical crack in thick-walled cylinder", *Engineering Fracture Mechanics*, Vol. 58, pp. 207–221, 1997.
4. Zheng, X.J., Glinka, G. and Dubey, R.N., "Calculation of stress intensity factors for semielliptical cracks in a thick-wall cylinder", *International Journal of Pressure Vessels and Piping*, Vol. 62, pp. 249–258, 1995.
5. Shen, G. and Glinka, G., "Weight functions for a surface semi-elliptical crack in a finite thickness plate", *Theoretical and Applied Fracture Mechanics*, Vol. 15, pp. 247–255, 1991.
6. Wang, X. and Lambert, S.B., "Stress intensity factors for low aspect ratio semi-elliptical surface cracks in finite-thickness plates subjected to nonuniform stresses", *Engineering Fracture Mechanics*, Vol. 51, pp. 517–532, 1995.
7. Wang, X. and Lambert, S.B., "Stress intensity factors and weight functions for high aspect ratio semi-elliptical surface cracks in finite-thickness plates", *Engineering Fracture Mechanics*, Vol. 57, pp. 13–24, 1997.
8. Wang, X. and Lambert, S.B., "Semi-elliptical surface cracks in finite-thickness plates with built-in ends. II. Weight function solutions", *Engineering Fracture Mechanics*, Vol. 68, pp. 1743–1754, 2001.
9. Beghini, M., Bertini, L. and Fontanari,V., "A weight function for 2D subsurface cracks under general loading conditions", *Engineering Fracture Mechanics*, Vol. 75, pp. 427–439, 2008.
10. Montenegro, H.L., Cisilino, A. and Otegui, J.L.",A weight function methodology for the assessment of embedded and surface irregular plane cracks", *Engineering Fracture Mechanics*, Vol. 73, pp. 2662–2684, 2006.
11. Anderson, T.L. and Glinka, G., "A closed-form method for integrating weight functions for part-through cracks subject to Mode I loading", *Engineering Fracture Mechanics*, Vol. 73, pp. 2153–2165, 2006.
12. Teh, L.S. and Brennan, F.P., "Evaluation of mode I stress intensity factors for edge cracks from 2-D V-notches using composition of constituent SIF weight functions", *International Journal of Fatigue*, Vol. 29, pp. 1253–1268, 2007.
13. Kim, J.H. and Lee, S.B., "Calculation of stress intensity factor using weight function method for a patched crack with debonding region", *Engineering Fracture Mechanics*, Vol. 67, pp. 303–310, 2000.
14. Guo, K., Bell, R. and Wang, X., "The stress intensity factor solutions for edge cracks in a padded plate geometry under general loading conditions", *International Journal of Fatigue*, Vol. 29, pp. 481–488, 2007.

15. Glinka, G. and Shen, G., "Universal features of weight functions for cracks in mode I", *Engineering Fracture Mechanics*, Vol. 40, pp. 1135–1146, 1991.
16. Newman, J.C. and Raju, I.S., "An empirical stress-intensity factor equation for the surface crack", *Engineering Fracture Mechanics*, Vol. 15, pp. 185–192, 1981.
17. Fett, T., Mattheck, C. and Munz, D., "On the calculation of crack opening displacement from the stress intensity factor", *Engineering Fracture Mechanics*, Vol. 27, pp. 697–715, 1987.
18. Raju, I.S. and Newman, J.C "Stress-intensity factors for internal and external surface cracks in cylindrical vessels", *Journal of Pressure Vessel Technology*, Vol. 104, pp. 293–298, 1982.